Supplementary information for Doping evolution of the charge excitations and electron correlations in electron-doped superconducting $La_{2-x}Ce_xCuO_4$

Jiaqi Lin,[1,2,3] Jie Yuan,[2] Kui Jin,[2,3] Zhiping Yin,[4,*] Gang Li,[1] Ke-Jin Zhou,[5] Xingye Lu,[4,6] Marcus Dantz,[6] Thorsten Schmitt,[6] Hong Ding,[2,3] Haizhong Guo,[7] Mark P. M. Dean,[8,†] and Xuerong Liu[1,‡]

[1] *School of Physical Science and Technology, ShanghaiTech University, Shanghai 201210, China*
[2] *Beijing National Laboratory for Condensed Matter Physics and Institute of Physics, Chinese Academy of Sciences, Beijing 100190, China*
[3] *University of Chinese Academy of Sciences, Beijing 100049, China*
[4] *Department of Physics and Center for Advanced Quantum Studies, Beijing Normal University, Beijing 100875, China*
[5] *Diamond Light Source, Harwell Science and Innovation Campus, Didcot, Oxfordshire OX11 0DE, United Kingdom*
[6] *Photon Science Division, Swiss Light Source, Paul Scherrer Institute, CH-5232 Villigen PSI, Switzerland*
[7] *School of Physical Engineering, Zhengzhou University, Zhengzhou 450001, China*
[8] *Department of Condensed Matter Physics and Materials Science, Brookhaven National Laboratory, Upton, New York 11973, USA*

(Dated: December 16, 2019)

* yinzhiping@bnu.edu.cn
† mdean@bnl.gov
‡ liuxr@shanghaitech.edu.cn

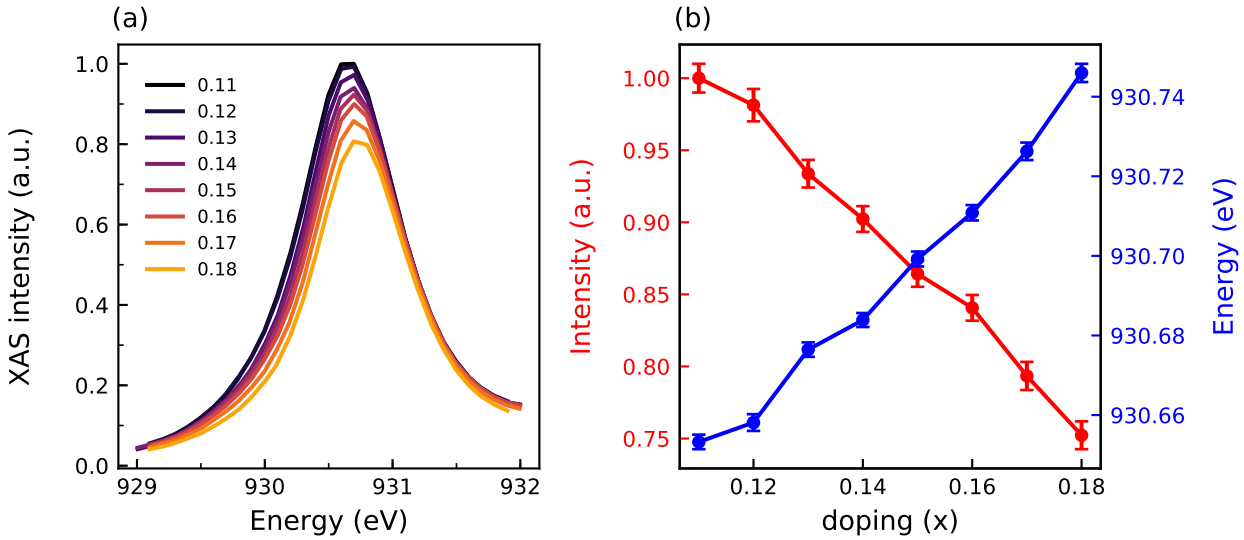

Supplementary Figure 1. Doping dependence of X-ray absorption spectroscopy (XAS) spectra of $La_{2-x}Ce_xCuO_4$ (LCCO) at Cu-L_3 edge. (a) XAS white line for x range of 0.11 to 0.18. (b) White line energy and intensity retrieved from fitting. Error bars describe the standard deviation from the least-squares fitting.

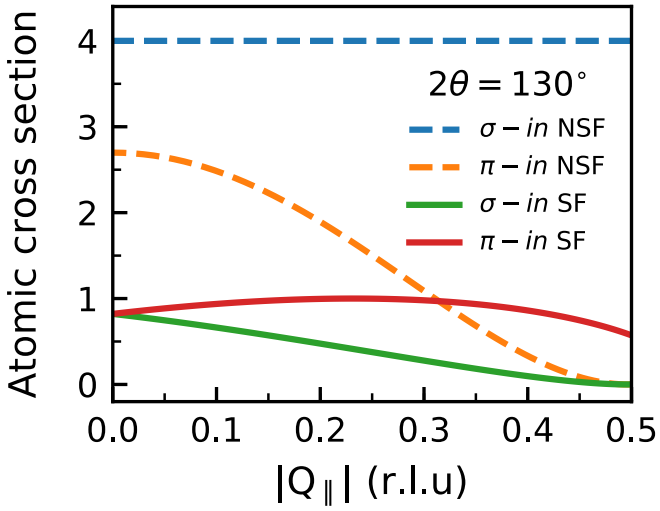

Supplementary Figure 2. RIXS spectra with incident beam polarization dependence. Atomic cross sections for π and σ incident beam polarization with grazing exit geometry at $2\theta = 130°$. The RIXS process at Cu L_3 edge can be written as $2p^6 3d^9 \rightarrow 2p^5 3d^{10} \rightarrow 2p^5 3d^{9*}$. This polarization related cross section calculates the ground state $d_{x^2-y^2} \downarrow$ to the final state $d_{x^2-y^2} \uparrow$ transition probability for the spin-flip component and non-spin-flip processes assuming that the spin direction lies in the CuO_2 plane.

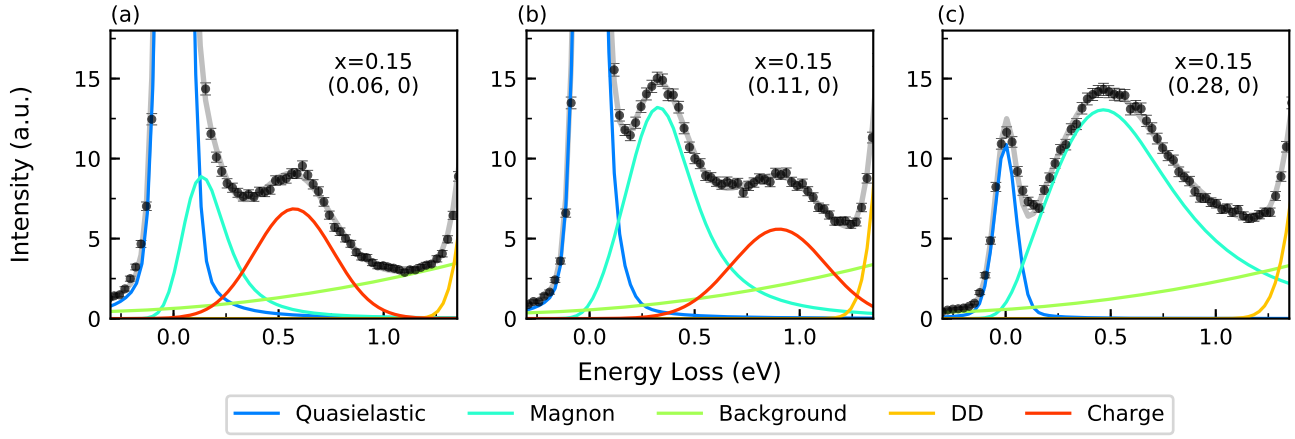

Supplementary Figure 3. Three typical RIXS spectra fitted with several components at doping x=0.15, for $q_{\parallel} = (0.06, 0)$, $(0.11, 0)$ and $(0.28, 0)$. The total RIXS spectrum is fitted with five components: A pseudo-Voigt function for the elastic line, an anti-symmetrized Lorentzian function multiplied by the Bose-Factor and convoluted with resolution function for the paramagnon, a Gaussian function convoluted with the resolution function for the plasmon and a Gaussian function for the *dd* excitations. Background scattering is treated with a polynominal function.

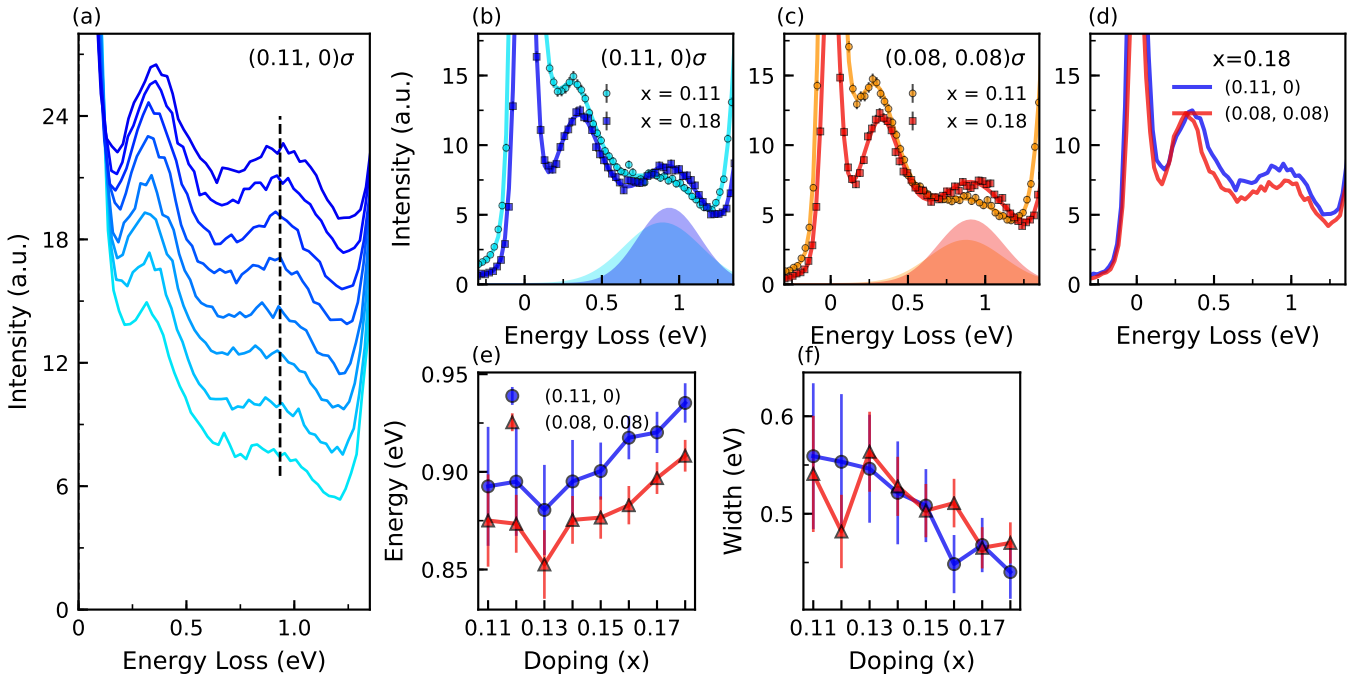

Supplementary Figure 4. Doping dependence of the plasmon. (a) RIXS spectra of LCCO at $\boldsymbol{Q} = (0.11, 0, 1.64)$ for $x = 0.11$ to 0.18. The vertical dashed line presents the plasmon energy for $x = 0.18$. Spectra are offset in vertical direction for clarity. (b,c) RIXS spectra at $\boldsymbol{Q} = (0.11, 0, 1.64)$ and (0.08, 0.08, 1.64). In each panel, spectra for $x = 0.11$ and $x = 0.18$ are compared. The shaded peaks show the Gaussian profile representing the plasmon. (d) RIXS spectra measured at $\boldsymbol{Q} = (0.11, 0, 1.64)$ and (0.08, 0.08, 1.64) show same dispersion with different in-plane directions $(H, 0)$ and (H, H) for $x = 0.18$. (e) Plasmon energy for each doping. (f) Plasmon full-width at half maximum (FWHM). Error bars describe the standard deviation from the least-squares fitting.

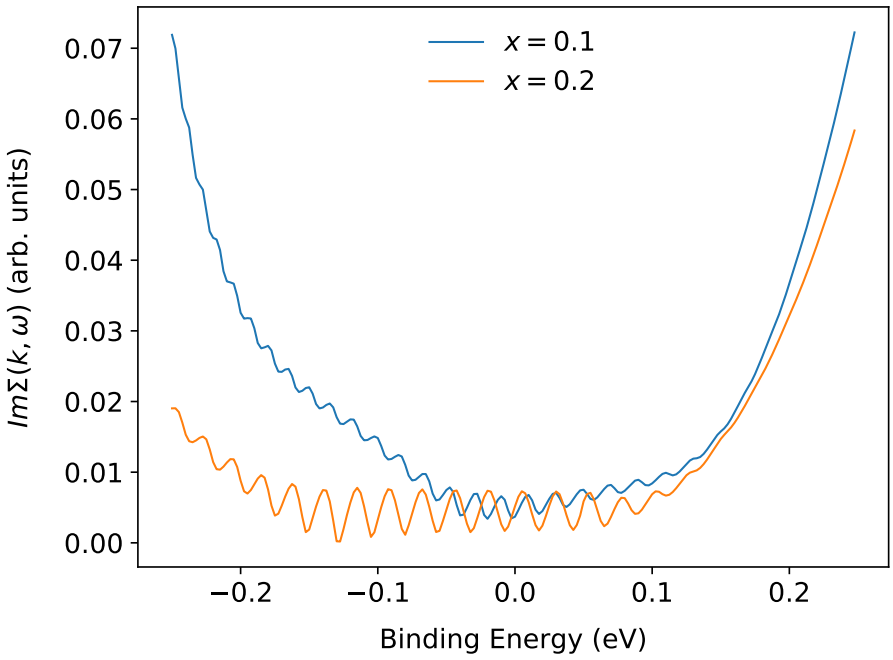

Supplementary Figure 5. Comparison of the imaginary part of the self-energy from the calculated single-particle spectral function for $x = 0.1$ and 0.2 along the $X - M$ direction. The wiggles near fermi level are artifacts from the fitting of momentum distribution curve (MDC) width.

SUPPLEMENTARY METHODS

DFT + DMFT calculation. We use density functional theory combined with dynamical mean field theory (DFT+DMFT) [1] to compute the electronic structure of electron-doped LCCO. The density functional theory part is based on the full-potential linear augmented plane wave method implemented in Wien2K [2] in conjunction with Perdew-Burke-Ernzerhof generalized gradient approximation [3] of the exchange correlation functional. DFT+DMFT is implemented on top of Wien2K and documented in [4]. In the DFT+DMFT calculations, the electronic charge is computed self-consistently on the DFT+DMFT density matrix. The quantum impurity problem is solved by the continuous time quantum Monte Carlo (CTQMC) method [5, 6] with Hubbard U=10.0 eV and Hund's coupling J=0.8 eV in the paramagnetic state at temperature of 116 K. The LCCO crystal structure (space group I4/mmm, #139) with lattice constants $a = b = 4.01$ Å and $c = 12.46$ Å is used in the calculations [7]. Virtual crystal approximation is employed to approximate the electron doping effect.

SUPPLEMENTARY DISCUSSION

Incident beam polarization dependence. Without resolving the scattered beam polarization, RIXS spectra contain both spin filp (SF) and non-spin filp (NSF) components for σ- or π-polarized incidence beam. Nevertheless, the relative contribution of SF and NSF components can be calculated through the single-site polarization dependent scattering matrix [8, 9]. In Supplementary Figure 2, we reproduce the atomic cross section with grazing exit geometry. For in-plane momentum transfer near the Brillouin zone (BZ) center, the NSF component has a larger cross section factor with σ polarized incident beam than π polarized, while the SF component behaviours oppositely. As shown in the main text Figure 2(a)-(b), we compare RIXS spectra for incident beams with σ and π polarization at several $q_{\parallel}$ points near the BZ center, focusing on the recently discovered mode in electron-doped cuprates. Through the comparison, RIXS spectra with σ-polarized incident beam consistently exhibit higher intensity than π-polarized incident beam, which indicates that the mode has NSF characteristics.

Electron correlation. From the single-particle spectral function, we know that the width of MDC is $Im\Sigma(k,\omega)/v_F$ [10]. $Im\Sigma(k,\omega)$ is the the imaginary part of the self-energy, which is inversely proportional to quasiparticle lifetime, v_F is the fermi velocity. We extract the MDC width and fermi velocity from the calculated single-particle spectral function in Figure 6 in main text, and plot the imaginary part of the self-energy in Supplementary Figure 5. It shows that the quasiparticle lifetime is longer in $x = 0.2$ than $x = 0.1$, especially at negative binding energies, which is directly related to electron correlation effect.

SUPPLEMENTARY REFERENCE

[1] Kotliar, G. et al. Electronic structure calculations with dynamical mean-field theory. *Rev. Mod. Phys.* **78**, 865–951 (2006).

[2] Blaha, P., Schwarz, K., Madsen, G. K., Kvasnicka, D. & Luitz, J. *Wien2k* TU Wien, Austria (2001).

[3] Perdew, J. P., Burke, K. & Ernzerhof, M. Generalized Gradient Approximation Made Simple. *Phys. Rev. Lett.* **77**, 3865 (1996).

[4] Haule, K., Yee, C. H. & Kim, K. Dynamical mean-field theory within the full-potential methods: Electronic structure of $CeIrIn_5$, $CeCoIn_5$, and $CeRhIn_5$ *Phys. Rev. B* **81**, 195107 (2010)

[5] Haule, K. Quantum Monte Carlo impurity solver for cluster dynamical mean-field theory and electronic structure calculations with adjustable cluster base. *Phy. Rev. B* **75**, 155113 (2007)

[6] Werber, P., Comanac, A., de' Medici, L., Troyer, M & Millis, A. J. Continuous-Time Solver for Quantum Impurity Models. *Phys. Rev. Lett.* **97**, 076405 (2006).

[7] Yu, H., Yuan, J., Zhu, B. & Jin, K. Manipulating composition gradient in cuprate superconducting thin films. *Sci. China Phys. Mech.* **60** 087421 (2017).

[8] Ament, L. J. P., Ghiringhelli, G., Sala, M. M, Braicovich, L. & van den Brink, J. Theoretical demonstration of how the dispersion of magnetic excitations in cuprate compounds can be determined using resonant inelastic x-ray scattering. *Phys. Rev. Lett.* **103**, 117003 (2009).

[9] Sala, M. M. et al. Energy and symmetry of dd excitations in undoped layered cuprates measured by Cu L_3 resonant inelastic x-ray scattering. *New J. Phys.* **13**, 043026 (2011).

[10] Armitage, N. P. et al, Angle-resolved photoemission spectral function analysis of the electron-doped cuprate $Nd_{1.85}Ce_{0.15}CuO_4$. *Phys. Rev. B 68*, 064517 (2003)